Application of transfer relations to structural analysis of arch bridges

Jiao-Long Zhang[1,2], Christian Hellmich[1], Herbert A. Mang[1,2],
Yong Yuan[2], Bernhard Pichler[1]

[1] *Institute for Mechanics of Materials and Structures*
TU Wien – Vienna University of Technology
Karlsplatz 13/202, A-1040 Vienna, Austria
e-mail: Bernhard.Pichler@tuwien.ac.at

[2] *College of Civil Engineering*
Tongji University
Siping Road 1239, 200092 Shanghai, China

Transfer relations, representing analytical solutions of the linear theory of slender circular arches, have facilitated structural analysis of segmented tunnel linings. This is the motivation to apply such relations to two examples of circular arch bridges in which the bridge deck is held from the arch by equally spaced hangers. First, the number of hangers is optimized to minimize the maximum bending moment of the arch, thus allowing the latter to come as close as possible to the desired thrust-line behavior. Next, analytical solutions for a "uniform temperature change" are derived and used to demonstrate that a temperature increase of 30 K results in minor redistributions of the inner forces but in significant additional deflections. The two examples have shown that the transfer relations are useful for structural analysis of circular arch bridges, because they reduce the complexity of the analysis to that of structural systems consisting of straight beams.

Keywords: segmented tunnel, predesign, first-order arch theory, transfer matrix.

NOMENCLATURE

A	–	cross-sectional area of the arch,
b	–	thickness of the cross-section,
$\mathbf{d}^a$	–	compliance vector of the arch with respect to a temperature change,
$\mathbf{d}^h$	–	compliance vector of hangers with respect to a temperature change,
d_p^a	–	p-th element of the compliance vector of the arch with respect to a temperature change,
d_p^h	–	p-th element of the compliance vector of the hangers with respect to a temperature change,
$\mathbf{e}_r, \mathbf{e}_\varphi$	–	base vectors,
EA	–	extensional stiffness of the arch,
EA_h	–	extensional stiffness of the hangers,
EI	–	bending stiffness of the arch,
EI_d	–	bending stiffness of the bridge deck,
F_p	–	support force acting at the p-th support,
H	–	rise of the arch,
I	–	second moment of the cross-sectional area,

$\mathbf{k}^d$ –   stiffness matrix of the deck,

k^d_{pq} –   element of $\mathbf{k}^d$,

ℓ –   horizontal distance between neighboring hangers,

l_p –   length of the p-th hanger,

L –   span of the arch,

M –   bending moment of the arch,

M_i –   bending moment at the initial cross-section of the arch,

M^L –   load integral for the bending moment,

M_p^{deck} –   bending moment of the deck at the connection with the p-th hanger,

n –   number of hangers,

N –   normal force of the arch,

N_i –   normal force at the initial cross-section of the arch,

N^L –   load integral for the normal force,

$\mathbf{P}$ –   point load imposed on the arch,

P_r –   radial component of the point load $\mathbf{P}$,

P_φ –   tangential component of the point load $\mathbf{P}$,

$\mathbf{P}_T$ –   vector of hanger forces induced by a temperature change,

$\mathbf{P}_p$ –   point load from the p-th hanger imposed on the arch,

P_p –   value of the point load $\mathbf{P}_p$,

P_{pr} –   radial component of the point load $\mathbf{P}_p$,

$P_{p\varphi}$ –   tangential component of the point load $\mathbf{P}_p$,

q –   dead load of the arch,

q_d –   dead load of the bridge deck,

q_h –   dead load of the hangers,

q_r –   distributed load in the radial direction,

q_φ –   distributed load in the tangential direction,

r –   radial coordinate of the polar coordinate system,

R –   radius of the axis of the circular arch,

S –   first moment of the area,

T_{ref} –   reference temperature referring to the time instant of completion of the construction of the arch,

$\mathbf{u}$ –   displacement vector of the axis,

u –   radial component of $\mathbf{u}$,

u_i –   radial displacement of the axis at the initial cross-section,

u^L –   load integral for the radial displacements,

V –   shear force,

v –   tangential component of $\mathbf{u}$,

v_i –   tangential displacement of the axis at the initial cross-section,

v^L –   load integral for the tangential displacements,

V_i –   shear force at the initial cross-section of the arch,

V^L –   load integral for the shear force,

x –   horizontal coordinate of the Cartesian coordinate system,

α_T –   coefficient of thermal expansion,

β –   inclination angle of the initial cross-section relative to the x-axis,

$\boldsymbol{\delta}^a$ –   compliance matrix of the arch with respect to point loads,

$\boldsymbol{\delta}^d$	–	compliance matrix of the deck with respect to hanger forces,
$\boldsymbol{\delta}^h$	–	compliance matrix of the hangers with respect to support forces,
δ^a_{pq}	–	element of $\boldsymbol{\delta}^a$,
δ^d_{pq}	–	element of $\boldsymbol{\delta}^d$,
δ^h_{pq}	–	element of $\boldsymbol{\delta}^h$,
ΔT	–	uniform temperature change relative to the reference temperature,
Δl_p	–	length change of the p-th hanger,
ε^e	–	eigenstrains,
γ	–	aperture angle of the circular arch,
$\omega_{a,p}$	–	vertical deflection of the arch at the connection with the p-th hanger,
$\omega_{d,p}$	–	vertical deflection of the deck at the connection with the p-th hanger,
σ	–	normal stress,
σ_v	–	von Mises stress,
τ	–	shear stress,
θ	–	cross-sectional rotation,
θ_i	–	rotation of the initial cross-section,
θ^L	–	load integral for the cross-sectional rotation,
φ	–	angular coordinate of the polar coordinate system,
φ_f	–	polar position of the final cross-section of the arch,
φ_i	–	polar position of the initial cross-section of the arch,
φ_p	–	polar position of a point load on the arch.

1. INTRODUCTION

Because of the curvature of arches, their structural analysis is more challenging and expensive than that of straight beams. Therefore, the development of methods facilitating structural analysis of arches is a topic of ongoing scientific research. Existing methods in bridge engineering include classical approaches, see, e.g., Fox [5], who reviewed the method of consistent deformations for pinned arches, representing structures that are statically indeterminate to the first degree, and Melbourne [8] who presented a method based on Castigliano's second theorem, according to which the partial derivative of the strain energy with respect to a force gives the displacement in the direction of this force. However, such analytical methods are easily applicable only to arches with low degrees of statical indeterminacy and specific types of external loads, as was shown by Dym [4] for arches with pinned or clamped supports under radial and gravitational line loads, as well as by Dym and Williams [2] for shallow arches subjected to a concentrated axial load acting at the end of the arch. As a remedy, most bridge designers use numerical methods, particularly for structural optimization [1, 7] and ultimate load analysis [10, 14]. However, the application of numerical methods may involve significant pre-processing efforts. This is the case, in particular, for sensitivity analysis of arch bridges, frequently involving several changes of the geometric dimensions of the arch and the number and arrangement of the hangers or the columns.

In order to improve this situation, transfer relations, representing analytical solutions of the linear theory of slender circular arches are considered herein. These relations are particularly valuable for hybrid analysis of displacement-monitored segmented tunnel rings, because they facilitate structural analysis of arches and allow for consideration of discontinuities of static and kinematic variables, resulting, e.g., from point loads and interfacial dislocations, respectively, in a straightforward manner [15]. This was the motivation to employ transfer relations also for structural analysis of arch bridges. The transfer relations used in this study are taken from [15]. They include solutions for unloaded parts of an arch, representing the main part of the transfer matrix, as well as

solutions for dead load and point loads, resulting in so-called *load integrals*. Load integrals for a uniform temperature change are, for the first time, reported in this paper. The transfer relations reduce the complexity of structural analysis of circular arches to the one encountered in systems consisting of straight beams. This is shown exemplarily by analyzing an arch bridge, consisting of a bridge deck, which is connected, via hangers, to two circular arches above. Two load cases are investigated: a dead load and a uniform temperature change.

The paper is organized as follows. Analytical solutions of the fundamental equations of the linear theory of slender circular arches and the corresponding transfer relations are presented in Sec. 2. Thereafter, these relations are applied to structural analysis of an arch bridge, including (i) sensitivity analysis with regard to the number of hangers and (ii) analysis of a uniform temperature rise in a statically indeterminate arch bridge, see Sec. 3. Results are discussed in Sec. 4. Conclusions are presented in Sec. 5.

2. Transfer relations: analytical solutions of the linear theory of slender circular arches

2.1. Governing equations

Slender arches with constant radius R, extensional stiffness EA, and bending stiffness EI, subjected to radial and tangential distributed loads, q_r and q_φ, are considered (Fig. 1). The governing equations, describing their mechanical behavior, involve six state variables: the cross-sectional rotation θ, the radial and the tangential displacement components of the axis of the arch, u and v, the normal force N, the shear force V, and the bending moment M. They read as [15]

$$\theta = \frac{1}{R}\frac{du}{d\varphi} - \frac{v}{R},\tag{1}$$

$$N = EA\left(\frac{u}{R} + \frac{1}{R}\frac{dv}{d\varphi} - \varepsilon^e\right),\tag{2}$$

$$M = -EI\left(\frac{1}{R^2}\frac{d^2u}{d\varphi^2} - \frac{1}{R^2}\frac{dv}{d\varphi}\right),\tag{3}$$
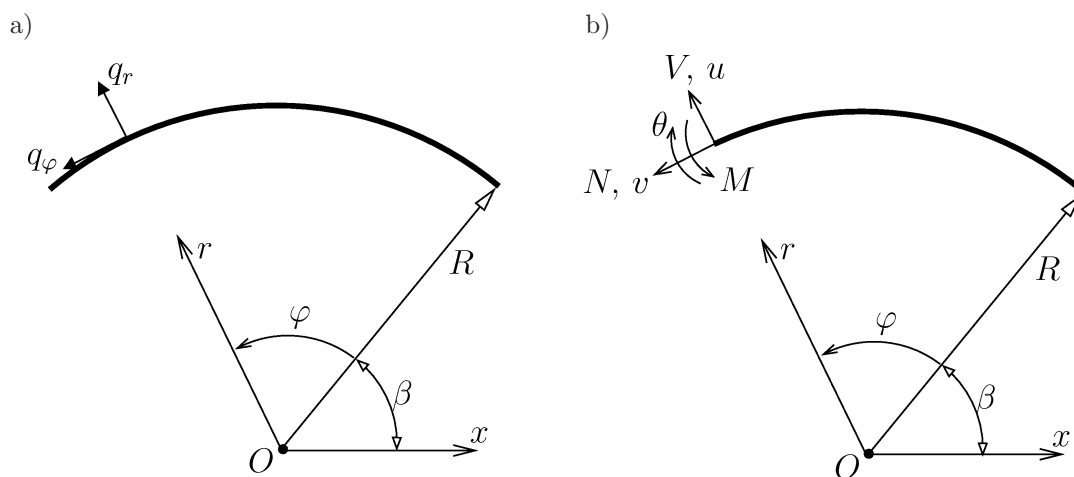
Fig. 1. a) Circular arch of radius R, loaded by radial and tangential distributed loads, q_r and q_φ, b) displacements and internal forces at an arbitrary cross-section; u and v denote the radial and the tangential component of the displacement of the axis, θ is the cross-sectional rotation, and N, M, and V are the normal force, the bending moment, and the shear force, respectively [15].

$$-\frac{N}{R} + \frac{1}{R}\frac{dV}{d\varphi} + q_r = 0, \tag{4}$$

$$\frac{1}{R}\frac{dN}{d\varphi} + \frac{V}{R} + q_\varphi = 0, \tag{5}$$

$$V - \frac{1}{R}\frac{dM}{d\varphi} = 0, \tag{6}$$

where ε^e denotes stress-free strains [11], also called eigenstrains [9]. These strains may, e.g., result from temperature changes.

The radial and tangential displacement components of the axis of the arch, u and v, provide access to the displacement field $\mathbf{u}$ as [3]

$$\mathbf{u} = u\,\mathbf{e}_r + \left[v - (r - R)\left(\frac{1}{R}\frac{du}{d\varphi} - \frac{v}{R}\right)\right]\mathbf{e}_\varphi, \tag{7}$$

where $\mathbf{e}_r$ and $\mathbf{e}_\varphi$ are base vectors in the radial and the tangential direction, respectively. Normal stresses σ and shear stresses τ are [6]

$$\sigma = \frac{N}{A} + \frac{M}{I}(r - R), \tag{8}$$

$$\tau = -\frac{V}{I}\frac{S}{b}, \tag{9}$$

where S is the first moment of area and b stands for the thickness of the cross-section in the direction normal to the axis.

2.2. Existing solutions for an unloaded part of the arch, for dead load, and for a point load [15]

Transfer relations are a "matrix-vector form" representation of analytical solutions of the set of differential equations (1)–(6). In more detail, the transfer relations relate the state vector at any tangential position φ to the vector of the state variables at the initial cross-section (index "i") by means of a matrix-vector product. These relations read as [15]

$$
\begin{bmatrix}
u(\varphi) \\
v(\varphi) \\
\theta(\varphi) \\
M(\varphi) \\
N(\varphi) \\
V(\varphi) \\
\hline
1
\end{bmatrix}
=
\left[
\begin{array}{cccccc:c}
\cos\varphi & \sin\varphi & T_{13}(\varphi) & T_{14}(\varphi) & T_{15}(\varphi) & T_{16}(\varphi) & \sum u^L(\varphi) \\
-\sin\varphi & \cos\varphi & T_{23}(\varphi) & T_{24}(\varphi) & T_{25}(\varphi) & T_{26}(\varphi) & \sum v^L(\varphi) \\
0 & 0 & 1 & T_{34}(\varphi) & T_{35}(\varphi) & T_{36}(\varphi) & \sum \theta^L(\varphi) \\
0 & 0 & 0 & 1 & T_{45}(\varphi) & T_{46}(\varphi) & \sum M^L(\varphi) \\
0 & 0 & 0 & 0 & \cos\varphi & -\sin\varphi & \sum N^L(\varphi) \\
0 & 0 & 0 & 0 & \sin\varphi & \cos\varphi & \sum V^L(\varphi) \\
\hdashline
0 & 0 & 0 & 0 & 0 & 0 & 1
\end{array}
\right]
\begin{bmatrix}
u_i \\
v_i \\
\theta_i \\
M_i \\
N_i \\
V_i \\
\hline
1
\end{bmatrix}, \tag{10}
$$

where

$$T_{13}(\varphi) = R \ \sin \varphi,$$

$$T_{14}(\varphi) = \frac{R^2}{EI}(\cos \varphi - 1),$$

$$T_{15}(\varphi) = \frac{R}{EA}\frac{1}{2}\varphi \sin \varphi + \frac{R^3}{EI}\left(\frac{1}{2}\varphi \sin \varphi + \cos \varphi - 1\right),$$

$$T_{16}(\varphi) = \frac{R}{EA}\left(\frac{1}{2}\varphi \cos \varphi - \frac{1}{2}\sin \varphi\right) + \frac{R^3}{EI}\left(\frac{1}{2}\varphi \cos \varphi - \frac{1}{2}\sin \varphi\right),$$

$$T_{23}(\varphi) = R \ (\cos \varphi - 1),$$

$$T_{24}(\varphi) = \frac{R^2}{EI}(\varphi - \sin \varphi),$$

$$T_{25}(\varphi) = \frac{R}{EA}\left(\frac{1}{2}\varphi \cos \varphi + \frac{1}{2}\sin \varphi\right) + \frac{R^3}{EI}\left(\varphi - \frac{3}{2}\sin \varphi + \frac{1}{2}\varphi \cos \varphi\right), \qquad (11)$$

$$T_{26}(\varphi) = \frac{R}{EA}\left(-\frac{1}{2}\varphi \sin \varphi\right) + \frac{R^3}{EI}\left(1 - \cos \varphi - \frac{1}{2}\varphi \sin \varphi\right),$$

$$T_{34}(\varphi) = -\frac{R}{EI}\varphi,$$

$$T_{35}(\varphi) = \frac{R^2}{EI}(\sin \varphi - \varphi),$$

$$T_{36}(\varphi) = \frac{R^2}{EI}(\cos \varphi - 1),$$

$$T_{45}(\varphi) = R \ (1 - \cos \varphi),$$

$$T_{46}(\varphi) = R \ \sin \varphi.$$

The top-left six-by-six submatrix of the transfer matrix in (10) represents the solution for an unloaded part of an arch, referring to the homogeneous solution of the differential equations (1)–(6). The top six elements of the last column of the transfer matrix refer to the superposition of all load integrals (marked by the superscript L). They represent solutions for external loads, such as dead load, point loads, and a uniform temperature change. The static and kinematic variables at the initial cross-section, u_i, v_i, θ_i, M_i, N_i, and V_i, represent integration constants that have to be determined with the help of boundary conditions.

The load integrals for dead load q read as [15]

$$u^L(\varphi) = \frac{R^2 q}{4EA}\left[\varphi^2 \sin(\varphi + \beta) + \varphi \cos(\varphi + \beta) - \cos \beta \sin \varphi\right]$$

$$+ \frac{R^4 q}{4EI}\left[\left(\varphi^2 - 4\right)\sin(\varphi + \beta) + 3\varphi \cos(\varphi + \beta) + 2\sin \varphi \cos \beta + 4\sin \beta\right], \quad (12)$$

$$v^L(\varphi) = \frac{R^2 q}{4EA} \left[\varphi^2 \cos(\varphi + \beta) + \varphi \sin(\varphi + \beta) - \sin \beta \sin \varphi \right]$$

$$+ \frac{R^4 q}{4EI} \left[\left(\varphi^2 - 8 \right) \cos(\varphi + \beta) - 5\varphi \sin(\varphi + \beta) + (\sin \varphi - 4\varphi) \sin \beta + 8 \cos \beta \right], \quad (13)$$

$$\theta^L(\varphi) = \frac{R^3 q}{EI} \left[\varphi \sin \beta + \varphi \sin(\varphi + \beta) + 2 \cos(\varphi + \beta) - 2 \cos \beta \right], \quad (14)$$

$$M^L(\varphi) = R^2 q \left[\sin(\varphi + \beta) - \varphi \cos(\varphi + \beta) - \sin \beta \right], \quad (15)$$

$$N^L(\varphi) = Rq\varphi \cos(\varphi + \beta), \quad (16)$$

$$V^L(\varphi) = Rq\varphi \sin(\varphi + \beta). \quad (17)$$

In Eqs. (12)–(17), β denotes the inclination angle of the initial cross-section relative to the x-axis, see Fig. 1.

The load integrals for the components P_r and P_φ of a point load $\mathbf{P}$, acting at the tangential position φ_p, read as [15]

$$u^L(\varphi) = \frac{1}{2} \frac{P_r R}{EA} \left[\sin(\varphi - \varphi_p) - (\varphi - \varphi_p) \cos(\varphi - \varphi_p) \right] H(\varphi - \varphi_p)$$

$$+ \frac{1}{2} \frac{P_\varphi R}{EA} \left[-(\varphi - \varphi_p) \sin(\varphi - \varphi_p) \right] H(\varphi - \varphi_p)$$

$$+ \frac{1}{2} \frac{P_r R^3}{EI} \left[\sin(\varphi - \varphi_p) - (\varphi - \varphi_p) \cos(\varphi - \varphi_p) \right] H(\varphi - \varphi_p)$$

$$+ \frac{1}{2} \frac{P_\varphi R^3}{EI} \left[-(\varphi - \varphi_p) \sin(\varphi - \varphi_p) - 2 \cos(\varphi - \varphi_p) + 2 \right] H(\varphi - \varphi_p), \quad (18)$$

$$v^L(\varphi) = \frac{P_r R}{EA} \left[\frac{1}{2} (\varphi - \varphi_p) \sin(\varphi - \varphi_p) \right] H(\varphi - \varphi_p)$$

$$+ \frac{P_\varphi R}{EA} \left[-\frac{1}{2} (\varphi - \varphi_p) \cos(\varphi - \varphi_p) - \frac{1}{2} \sin(\varphi - \varphi_p) \right] H(\varphi - \varphi_p)$$

$$+ \frac{P_r R^3}{EI} \left[\frac{1}{2} (\varphi - \varphi_p) \sin(\varphi - \varphi_p) + \cos(\varphi - \varphi_p) - 1 \right] H(\varphi - \varphi_p)$$

$$+ \frac{P_\varphi R^3}{EI} \left[\frac{3}{2} \sin(\varphi - \varphi_p) - \frac{1}{2} (\varphi - \varphi_p) \cos(\varphi - \varphi_p) - (\varphi - \varphi_p) \right] H(\varphi - \varphi_p), \quad (19)$$

$$\theta^L(\varphi) = \frac{P_r R^2}{EI} \left[1 - \cos(\varphi - \varphi_p) \right] H(\varphi - \varphi_p) - \frac{P_\varphi R^2}{EI} \left[\sin(\varphi - \varphi_p) - (\varphi - \varphi_p) \right] H(\varphi - \varphi_p), \quad (20)$$

$$M^L(\varphi) = -R \left\{ P_r \sin(\varphi - \varphi_p) + P_\varphi \left[1 - \cos(\varphi - \varphi_p) \right] \right\} H(\varphi - \varphi_p), \quad (21)$$

$$N^L(\varphi) = \left[P_r \sin(\varphi - \varphi_p) - P_\varphi \cos(\varphi - \varphi_p) \right] H(\varphi - \varphi_p), \quad (22)$$

$$V^L(\varphi) = - \left[P_r \cos(\varphi - \varphi_p) + P_\varphi \sin(\varphi - \varphi_p) \right] H(\varphi - \varphi_p). \quad (23)$$

In Eqs. (18)–(23), $H(\varphi - \varphi_p)$ stands for the Heaviside function.

2.3. Deriving load integrals for a uniform temperature change

A *uniform* temperature change ΔT relative to a reference temperature T_{ref} is considered. T_{ref} refers to the time instant of completion of the construction of the arch. By denoting the thermal expansion coefficient of the arch material as α_T, the load variables read as

$$\varepsilon^e = \alpha_T \Delta T, \tag{24}$$

$$q_r = q_\varphi = 0. \tag{25}$$

The corresponding load integrals $N^L(\varphi)$, $V^L(\varphi)$, and $M^L(\varphi)$ follow from the coupled system of differential equations obtained by specializing Eqs. (4)–(6) for Eqs. (24) and (25):

$$\begin{bmatrix} 0 & -\dfrac{1}{R} & \dfrac{1}{R}\dfrac{d}{d\varphi} \\[2mm] 0 & \dfrac{1}{R}\dfrac{d}{d\varphi} & \dfrac{1}{R} \\[2mm] -\dfrac{1}{R}\dfrac{d}{d\varphi} & 0 & 1 \end{bmatrix} \begin{bmatrix} M^L \\[2mm] N^L \\[2mm] V^L \end{bmatrix} = \begin{bmatrix} 0 \\[2mm] 0 \\[2mm] 0 \end{bmatrix}. \tag{26}$$

Solving the above system of differential equations by considering homogeneous boundary conditions $N^L(0) = V^L(0) = M^L(0) = 0$, see [15], delivers

$$N^L(\varphi) = V^L(\varphi) = M^L(\varphi) = 0. \tag{27}$$

The load integrals $u^L(\varphi)$, $v^L(\varphi)$, and $\theta^L(\varphi)$ follow from the coupled system of differential equations obtained by specializing Eqs. (1)–(3) for Eqs. (24) and (27):

$$\begin{bmatrix} \dfrac{1}{R}\dfrac{d}{d\varphi} & -\dfrac{1}{R} & -1 \\[2mm] \dfrac{1}{R} & \dfrac{1}{R}\dfrac{d}{d\varphi} & 0 \\[2mm] \dfrac{d^2}{d\varphi^2} & -\dfrac{d}{d\varphi} & 0 \end{bmatrix} \begin{bmatrix} u^L \\[2mm] v^L \\[2mm] \theta^L \end{bmatrix} = \begin{bmatrix} 0 \\[2mm] \alpha_T \Delta T \\[2mm] 0 \end{bmatrix}. \tag{28}$$

Solving the above system of differential equations by considering homogeneous boundary conditions $u^L(0) = v^L(0) = \theta^L(0) = 0$, see [15], delivers

$$u^L(\varphi) = \alpha_T \, \Delta T \, R(1 - \cos\varphi), \tag{29}$$

$$v^L(\varphi) = \alpha_T \, \Delta T \, R, \tag{30}$$

$$\theta^L(\varphi) = 0. \tag{31}$$

2.4. Determination of the integration constants from boundary conditions

The six integration constants, see u_i, v_i, θ_i, M_i, N_i, and V_i in Eq. (10), are determined by means of six boundary conditions. Three of them refer to the support conditions at the initial cross-section of the arch and the remaining three to its final cross-section (index "f"). The three boundary conditions at the initial cross-section of the arch provide direct access to three integration constants. The remaining three integration constants follow from the formulation of boundary conditions at the final cross-section. This requires a relationship between the state variables at the initial and the final cross-section of the arch. To this end, the transfer relations (10) are specified for $\varphi = \varphi_f$ such that the vector on the left-hand side of (10) contains the state variables at the final cross-section of the arch. Considering the three boundary conditions in this vector delivers three algebraic equations for the remaining three integration constants. After obtaining the integration constants, the state variables at any cross-section of interest can be determined simply by evaluating the transfer relations (10) for the corresponding value of φ.

3. Exemplary structural analysis of an arch bridge

The transfer relations (10) are used for structural analysis of an arch bridge similar to the one investigated in [12]. The considered bridge consists of two parallel circular arches, carrying the bridge deck via two pairs of equally-spaced vertical hangers, see Fig. 2a. Both arches are circular box girders, resting on pinned supports. Therefore, the boundary conditions are as follows:

$$\left.\begin{array}{c} \varphi = 0 \\ \varphi = \varphi_f \end{array}\right\} : \quad u = v = M = 0. \tag{32}$$
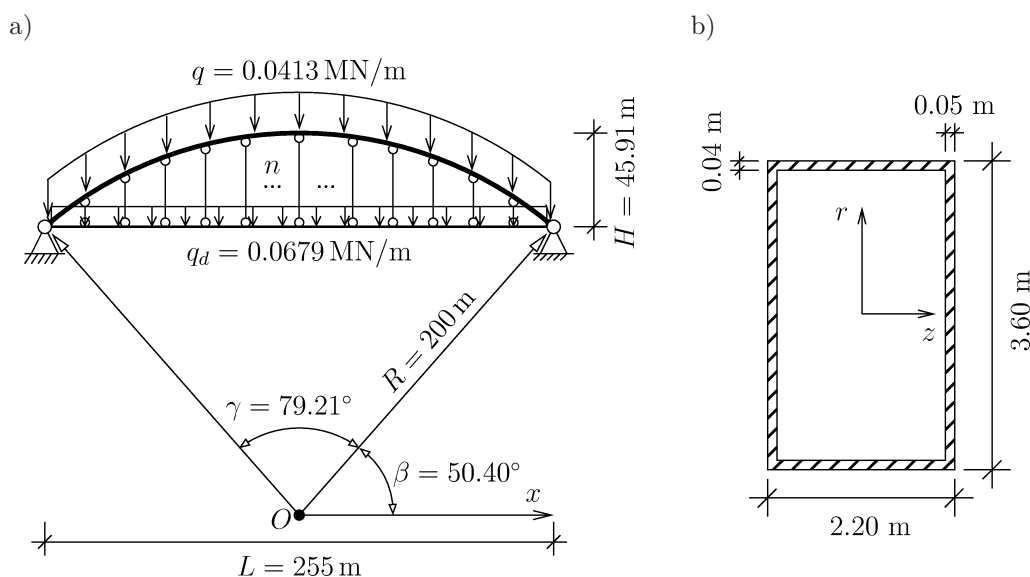
Fig. 2. Through arch bridge: a) dimensions of the bridge and distributed dead-load of both the arch and the deck, b) cross-section of the arch.

The width of the cross-sections of the steel arches is 2.20 m and the height is 3.60 m, see Fig. 2b. The thickness of the flanges and the webs is 0.04 m and 0.05 m, respectively. Thus, the extensional stiffness EA, the bending stiffness EI, and the dead load q of each of the two arches are obtained as

$$EA = 110460 \text{ MN}, \tag{33}$$

$$EI = 191478 \text{ MNm}^2, \tag{34}$$

$$q = 0.0413 \text{ MN/m}. \tag{35}$$

The span L and the radius R of the arches, see also Fig. 2a, are given as

$$L = 255 \text{ m}, \tag{36}$$

$$R = 200 \text{ m}. \tag{37}$$

Thus, the rise of the arch is $H = 45.91$ m. The aperture angle $\gamma(= \varphi_f)$ is equal to 79.21°, see Fig. 2a. The inclination angle β of the initial cross-section is equal to 50.40°. In the following, *one half* of the bridge is analyzed. It consists of one arch, one half of the bridge deck, and the connecting hangers.

The bridge deck is simply supported at both ends. It is connected to the arches above via two pairs of n hangers. Consistent with the investigation of one half of the bridge, the dead load q_d and the bending stiffness EI_d refer to one half of the bridge deck. Thus,

$$q_d = 0.0679 \text{ MN/m} \tag{38}$$

and

$$EI_d = 574434 \text{ MNm}^2. \tag{39}$$

All hangers have the same cross-sectional properties. The dead load q_h and the extensional stiffness EA_h are given as

$$q_h = 0.0025 \text{ MN/m} \tag{40}$$

and

$$EA_h = 6597 \text{ MN}. \tag{41}$$

The thermal expansion coefficient of steel is given as

$$\alpha_T = 10.8 \cdot 10^{-6} \text{ K}^{-1}. \tag{42}$$

In the following, the sensitivity of the load-carrying behavior of the arch with respect to the number of equally spaced hangers will be investigated, considering the dead load of the arch, the hangers, and the bridge deck, see Subsec. 3.1. Thereafter, a uniform temperature change of the structure will be considered. This involves quantification of the redistribution of the internal forces and of changes of the deformations of the arch, see Subsec. 3.2.

3.1. Sensitivity of the response of the arch with respect to the number of hangers

Considering the dead load of the arch, the bridge deck, and the hangers, the maximum bending moments of the arch are computed as a function of the number of the hangers, n. The horizontal distance between neighboring hangers ℓ is given as

$$\ell = \frac{L}{n}. \tag{43}$$

The length of the p-th hanger is obtained as

$$l_p = \sqrt{R^2 - (p\ell - L/2)^2} - R\sin\beta. \tag{44}$$

The hanger forces depend on the construction strategy. Typically, the lengths of the hangers are adjusted so that the deck deflections vanish at the positions of the hangers. In other words, the deck behaves like a continuous beam with n intermediate supports, see Fig. 3a. The support forces of this beam are equal to the forces imposed from the bridge deck on the hangers. Determination of these forces represents a problem that is statically indeterminate to the n-th degree. It is solved by means of Clapeyron's three-moments equations [13]. The statically indeterminate forces are chosen as the bending moments of the deck at the positions of the intermediate supports, see Fig. 3b. Formulation of the three-moments equation for the p-th intermediate support gives

$$\frac{\ell}{6}M_{p-1}^{\text{deck}} + \frac{2\ell}{3}M_p^{\text{deck}} + \frac{\ell}{6}M_{p+1}^{\text{deck}} = -\frac{q_d\ell^3}{12}. \tag{45}$$

a)

b)

c)
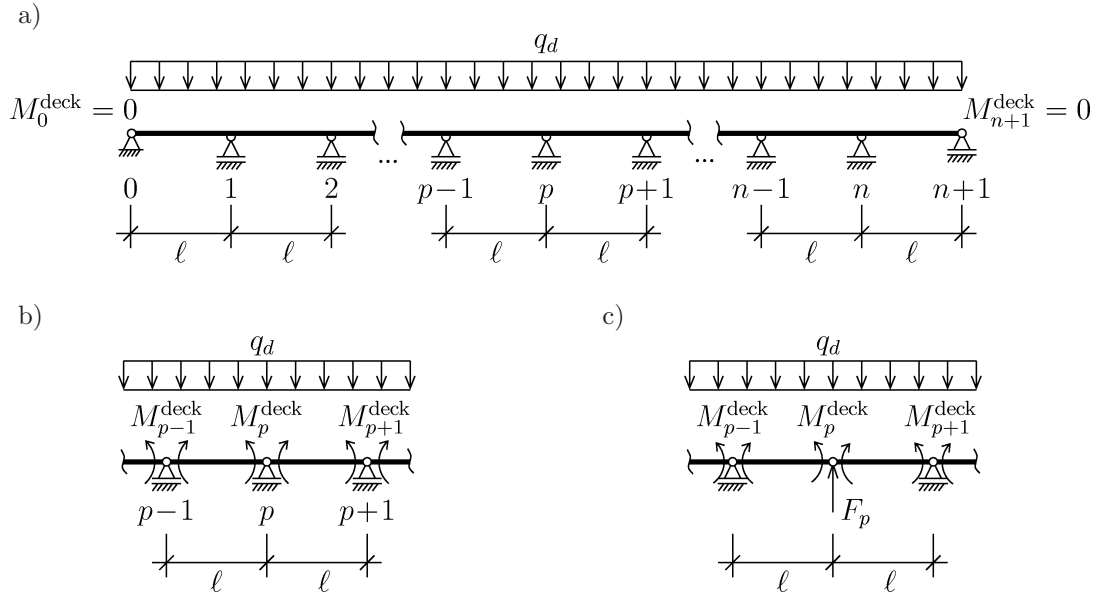
Fig. 3. Structural analysis of the deck: a) statically indeterminate continuous beam with n intermediate supports, b) three neighboring supports in the context of Clapeyron's three-moments equations, and c) support force F_p.

Formulation of n deformation conditions according to (45) results in the following system of linear algebraic equations for the bending moments M_p^{deck}, $p = 1, 2, \ldots, n$:

$$
\begin{bmatrix}
4 & 1 & 0 & 0 & \cdots & 0 & 0 & 0 & 0 \\
1 & 4 & 1 & 0 & \cdots & 0 & 0 & 0 & 0 \\
0 & 1 & 4 & 1 & \cdots & 0 & 0 & 0 & 0 \\
\vdots & \vdots & \vdots & \vdots & & \vdots & \vdots & \vdots & \vdots \\
0 & 0 & 0 & 0 & \cdots & 1 & 4 & 1 & 0 \\
0 & 0 & 0 & 0 & \cdots & 0 & 1 & 4 & 1 \\
0 & 0 & 0 & 0 & \cdots & 0 & 0 & 1 & 4
\end{bmatrix}
\begin{bmatrix}
M_1^{\text{deck}} \\
M_2^{\text{deck}} \\
M_3^{\text{deck}} \\
\vdots \\
M_{n-2}^{\text{deck}} \\
M_{n-1}^{\text{deck}} \\
M_n^{\text{deck}}
\end{bmatrix}
= -\frac{q_d \ell^2}{2}
\begin{bmatrix}
1 \\
1 \\
1 \\
\vdots \\
1 \\
1 \\
1
\end{bmatrix}.
\tag{46}
$$

After solving (46), the support forces follow from equilibrium considerations as

$$
F_p = q_d \ell + \frac{M_{p-1}^{\text{deck}} - 2M_p^{\text{deck}} + M_{p+1}^{\text{deck}}}{\ell}, \qquad p = 1, 2, \ldots, n,
\tag{47}
$$

see also Fig. 3c. Adding the dead load of the hangers to F_p yields the hanger forces as

$$
P_p = F_p + q_h l_p.
\tag{48}
$$

For determination of the corresponding load integrals, see (18)–(23), the hanger forces are decomposed into their radial and tangential components. This requires knowledge of the position angle φ_p. This angle is obtained as (see also Fig. 4)

$$
\varphi_p = \arccos\left(\frac{p\,\ell - L/2}{R}\right) - \beta, \qquad p = 1, 2, \ldots, n.
\tag{49}
$$
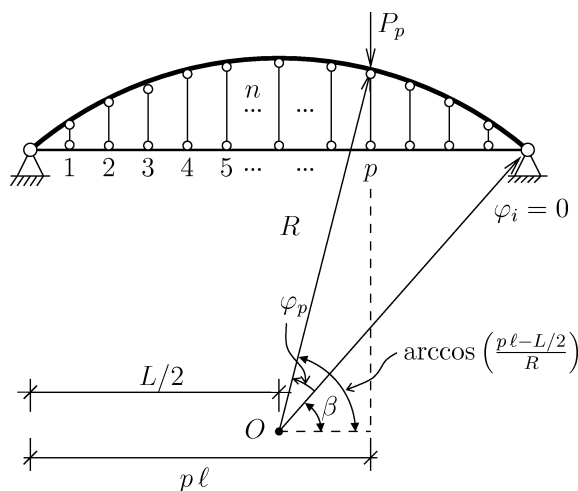
Fig. 4. Polar position φ_p of hanger force P_p.

The radial and the tangential components of the hanger force $\mathbf{P}_p$ are obtained as

$$P_{pr} = -P_p \sin(\varphi_p + \beta), \tag{50}$$

$$P_{p\varphi} = -P_p \cos(\varphi_p + \beta), \qquad p = 1, 2, \ldots, n. \tag{51}$$

Structural analysis of the arch with n hangers is accomplished by means of the transfer relations (10). At first, the transfer matrix is formulated for the set of load integrals that refer to the dead load of the arch, see (12)–(17), and for n sets of load integrals, referring to n different point loads at n positions, see (18)–(23), such that the summation symbols in the last column of the transfer matrix (10) extend over $n + 1$ load cases. The resulting transfer relations are specialized for the numerical values of the stiffness and the dead load of the arch, see (33)–(35), its radius, see (37), and for point loads and their positions, obtained from the combination of (36)–(38), (40), and (43)–(51). Finally, the integration constants are determined by means of the boundary conditions (32), as described in Subsec. 2.4. Thereafter, the transfer relations can be simply evaluated for any cross-section in order to quantify the static and kinematic variables of the arch.

The described mode of structural analysis is repeated 49 times in order to study 50 arch bridges, differing in the number of hangers from $n = 1$ to $n = 50$. From the 50 solutions, the maximum bending moments $\max_\varphi |M(\varphi, n)|$ are determined, see Fig. 5. Using the maximum bending moment of the arch in the special case of just one hanger ($n = 1$) as the reference, the maximum bending moment
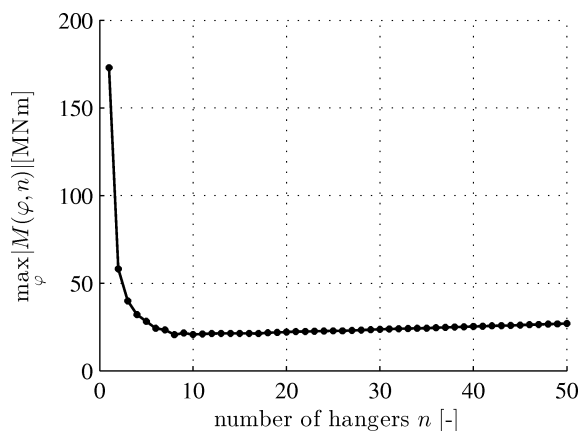
Fig. 5. Maximum bending moment of an arch as a function of the number of hangers.

decreases by 88% if the hanger number is increased up to $n = 8$. A further increase of the hanger number, however, results in a moderate increase of the maximum bending moment.

Similar results are obtained from stress analysis. The normal stress, σ, is computed from the normal force and the bending moment, see (8). The shear stress, τ, is obtained from the shear force, see (9). Knowledge of σ and τ allows for determination of the von Mises stress:

$$\sigma_v = \sqrt{\sigma^2 + 3\,\tau^2}. \tag{52}$$

Increasing the hanger number from 1 to 3, and further to 8 and 30, results in a change of the maximum von Mises stress from 378 MPa to 122 MPa, 86 MPa, and 93 MPa, the maximum displacement from 0.704 m to 0.198 m, 0.171 m, and 0.196 m, and the maximum cross-sectional rotation from 0.0163 rad to 0.0045 rad, 0.0032 rad, and 0.0037 rad, see Fig. 6. The obtained results will be discussed in more detail in Sec. 4.
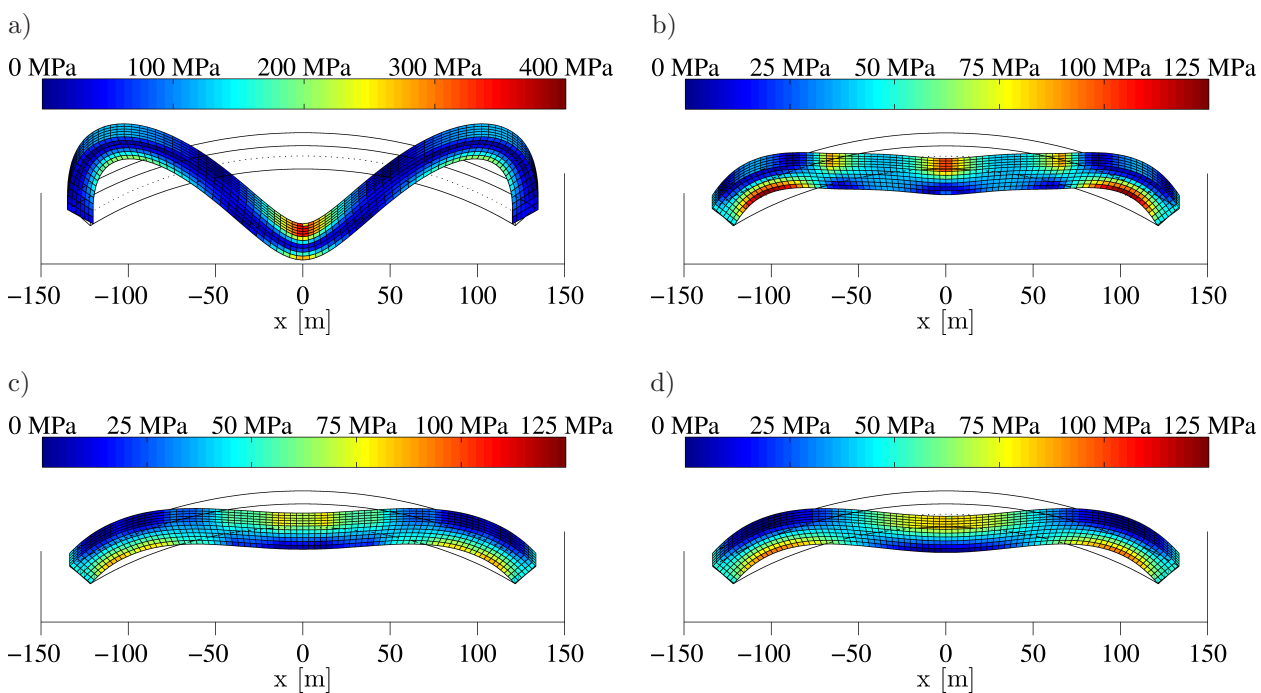
Fig. 6. Distribution of the von Mises stress in the deformed configuration of the arches with different numbers of hangers: a) $n = 1$, b) $n = 3$, c) $n = 8$, d) $n = 30$; the magnification factors of the cross-sectional dimensions and the displacements are 5 and 100, respectively.

3.2. Uniform temperature change of the structure

The arch bridge is loaded by a uniform temperature change ΔT. Determination of the resulting hanger forces requires formulation of n deformation conditions. The p-th condition involves (i) the vertical deflection of the arch at the connection with the p-th hanger $\omega_{a,p}$, (ii) the change of the hanger length Δl_p, and (iii) the deflection of the deck at the connection with the p-th hanger $\omega_{d,p}$. Defining the vertical deflections $\omega_{a,p}$ and $\omega_{d,p}$ as positive when oriented downward, the deformation conditions read as

$$\omega_{a,p} + \Delta l_p = \omega_{d,p}, \qquad p = 1, 2, \ldots, n. \tag{53}$$

The vertical arch displacements follow from the radial and the tangential displacement components as

$$\omega_{a,p} = -u(\varphi_p)\sin(\beta + \varphi_p) - v(\varphi_p)\cos(\beta + \varphi_p), \qquad p = 1, 2, \ldots, n. \tag{54}$$

The vertical arch displacements are functions of the temperature change and of the hanger forces resulting from the temperature change:

$$\omega_{a,p} = \sum_{q=1}^{n} \delta_{pq}^{a} P_q + d_p^a \Delta T, \qquad p = 1, 2, \dots n, \tag{55}$$

where δ_{pq}^{a} is an element of an $n \times n$ compliance matrix, d_p^a is an element of an n-dimensional compliance vector, and P_q is an element of an n-dimensional vector, $\mathbf{P}_T$ (the subscript T stands for the temperature change), containing the sought hanger forces. In order to compute the compliances occurring in (55), it is noted that δ_{pq}^{a} is equal to the vertical displacement $\omega_{a,p}$ resulting from $P_q = 1$ MN, whereas all other hanger forces and ΔT are equal to zero. It is also noted that d_p^a is equal to the vertical displacement $\omega_{a,p}$ if all P_q are equal to zero and $\Delta T = 1$ K. Therefore, $(n+1)$ load cases of the arch are treated, using the transfer relations. Load case 1 consists of a vertical unit point load at the connection of hanger 1 to the arch, load case 2 consists of a vertical unit point load at the connection of hanger 2 to the arch, and so on. The $(n+1)$-st load case is the uniform temperature change. For all load cases, the displacement components u and v are computed at all points connecting the arch with the hangers. This allows for computation of the arch displacements $\omega_{a,p}$, see (54).

The length changes of the hangers contain two contributions. The first one is related to the hanger forces P_p and the second one to the temperature change ΔT

$$\Delta l_p = \frac{l_p}{EA_h} P_p + l_p \alpha_T \Delta T, \qquad p = 1, 2, \dots, n. \tag{56}$$

Analogous to (55), the length changes of the hangers Δl_p can be expressed as

$$\Delta l_p = \sum_{q=1}^{n} \delta_{pq}^{h} P_q + d_p^h \Delta T, \qquad p = 1, 2, \dots, n, \tag{57}$$

where $\delta_{pp}^{h} = l_p/EA_h$ with $\delta_{pq}^{h} = 0$, $p \neq q$, and $d_p^h = l_p \alpha_T$.

The deflections of the deck at the connections with the hangers are functions of the hanger forces, given as

$$\omega_{d,p} = \sum_{q=1}^{n} \delta_{pq}^{d} P_q, \qquad p = 1, 2, \dots, n, \tag{58}$$

where δ_{pq}^{d} represents an element of an $n \times n$ compliance matrix. This matrix is obtained with the help of Clapeyron's three-moments equations, considering displacements which are imposed at the supports of a continuous beam (see also Fig. 7). This yields

$$\frac{\ell}{6} M_{p-1}^{\text{deck}} + \frac{2\ell}{3} M_p^{\text{deck}} + \frac{\ell}{6} M_{p+1}^{\text{deck}} = -\frac{\omega_{d,p-1} - 2\,\omega_{d,p} + \omega_{d,p+1}}{\ell} EI_d, \qquad p = 1, 2, \dots, n. \tag{59}$$
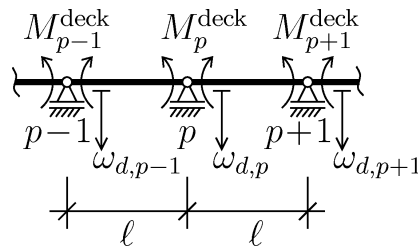
Fig. 7. Displacements imposed at the supports within the framework of Clapeyron's three-moments equations.

Formulation of (59) for all intermediate supports and solution for the bending moments result in

$$
\begin{bmatrix} M_1^{\text{deck}} \\ M_2^{\text{deck}} \\ M_3^{\text{deck}} \\ \vdots \\ M_{n-2}^{\text{deck}} \\ M_{n-1}^{\text{deck}} \\ M_n^{\text{deck}} \end{bmatrix} = -
\begin{bmatrix}
4 & 1 & 0 & 0 & \cdots & 0 & 0 & 0 & 0 \\
1 & 4 & 1 & 0 & \cdots & 0 & 0 & 0 & 0 \\
0 & 1 & 4 & 1 & \cdots & 0 & 0 & 0 & 0 \\
\vdots & \vdots & \vdots & \vdots & & \vdots & \vdots & \vdots & \vdots \\
0 & 0 & 0 & 0 & \cdots & 1 & 4 & 1 & 0 \\
0 & 0 & 0 & 0 & \cdots & 0 & 1 & 4 & 1 \\
0 & 0 & 0 & 0 & \cdots & 0 & 0 & 1 & 4
\end{bmatrix}^{-1}
\begin{bmatrix}
0 & -2\omega_{d,1} & +\omega_{d,2} \\
\omega_{d,1} & -2\omega_{d,2} & +\omega_{d,3} \\
\omega_{d,2} & -2\omega_{d,3} & +\omega_{d,4} \\
& \vdots & \\
\omega_{d,n-3} & -2\omega_{d,n-2} & +\omega_{d,n-1} \\
\omega_{d,n-2} & -2\omega_{d,n-1} & +\omega_{d,n} \\
\omega_{d,n-1} & -2\omega_{d,n} & +0
\end{bmatrix} \frac{6EI_d}{\ell^2}.
\tag{60}
$$

In the present case of temperature loading, the support forces are equal to the hanger forces. Analogous to (47), they follow as

$$
P_p = \frac{M_{p-1}^{\text{deck}} - 2M_p^{\text{deck}} + M_{p+1}^{\text{deck}}}{\ell}, \qquad p = 1, 2, \ldots, n.
\tag{61}
$$

Inserting the bending moments (60) into (61) gives

$$
P_p = \sum_{q=1}^{n} k_{pq}^d \omega_{d,q}, \qquad p = 1, 2, \ldots, n,
\tag{62}
$$

where k_{pq}^d denotes a known element of the $n \times n$ stiffness matrix. Rewriting (62) in symbolic notation gives

$$
\mathbf{P}_T = \mathbf{k}^d \cdot \boldsymbol{\omega}_d.
\tag{63}
$$

Solving this system of linear equations for $\boldsymbol{\omega}_d$ yields

$$
\boldsymbol{\omega}_d = \left[\mathbf{k}^d \right]^{-1} \cdot \mathbf{P}_T = \boldsymbol{\delta}^d \cdot \mathbf{P}_T,
\tag{64}
$$

where $\boldsymbol{\delta}^d$ denotes the compliance matrix according to (58).

In order to compute the sought hanger forces, (55), (57), and (58) are inserted into (53). Using symbolic notation, this gives

$$
\boldsymbol{\delta}^a \cdot \mathbf{P}_T + \mathbf{d}^a \Delta T + \boldsymbol{\delta}^h \cdot \mathbf{P}_T + \mathbf{d}^h \Delta T = \boldsymbol{\delta}^d \cdot \mathbf{P}_T.
\tag{65}
$$

Solving (65) for the vector of hanger forces yields

$$
\mathbf{P}_T = \left[\boldsymbol{\delta}^d - \boldsymbol{\delta}^a - \boldsymbol{\delta}^h \right]^{-1} \cdot \left[\mathbf{d}^a + \mathbf{d}^h \right] \Delta T.
\tag{66}
$$

As an example, an arch bridge with the optimum number of hangers, $n = 8$, and a uniform temperature change of

$$
\Delta T = 30 \text{ K}
\tag{67}
$$

is considered. The maximum values of the von Mises stress, the displacement, and the cross-sectional rotations are 5 MPa, 0.102 m, and 0.0011 rad, respectively, see also Fig. 8. Comparing these results with the ones from the load case *dead load*, characterized by the maximum value of the von Mises stress of 86 MPa, the displacements of 0.171 m, and the cross-sectional rotations of 0.0032 rad, it is seen that a uniform temperature change of 30 K results in rather small redistributions of the load but in a significant change of the deformed configuration.
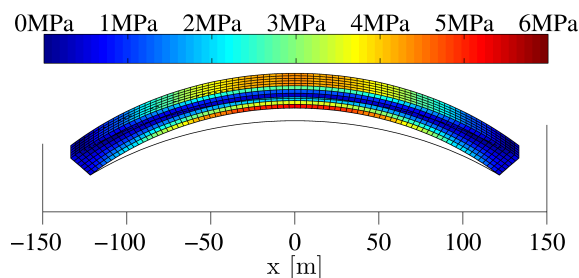
Fig. 8. Distribution of von Mises stresses induced by a uniform temperature change of $\Delta T = 30$ K; the magnification factors of the cross-sectional dimensions and the displacements are 5 and 100, respectively.

4. DISCUSSION

The connection of a bridge deck to the arch via hangers results in bending of the arch. The maximum bending moment can be minimized by choosing the optimum number of hangers. The existence of such an optimum for the load case dead load is the consequence of two counteracting effects. Increasing the number of hangers results in:

1) less concentrated loading of the arch, entailing a reduction of the maximum bending moment, and

2) an increase of the total hanger mass and, therefore, in an increase of the loading of the arch, resulting in an increase of the maximum bending moment.

With regard to the investigated bridge, it was found that an increase of the number of hangers up to eight results in a reduction of the maximum bending moment. If this number is further increased, the increase of the maximum bending moment due to the increased mass of the hangers overcompensates the reduction of the maximum bending moment, caused by the improved distribution of the deck weight.

The derived transfer relations are not restricted to arch bridges with *vertical* hangers and *pinned supports*. They can be also used for any arrangement of the hangers, provided that the radial and the tangential components of the point loads are known. These relations can also be used for arbitrary support conditions.

The transfer relations are appealing for structural analysis of arch bridges. This conclusion is based on the following findings:

- The transfer relations reduce the amount of preprocessing in a comparative analysis of bridges that differ in the number of hangers, because there are no discretization efforts. Hanger forces and their load points are considered simply via corresponding load integrals. This is different from mesh-based numerical simulation methods, where each connection of a hanger to the arch requires node-to-node connectivity. In other words, the discretization of an arch must be customized for specific hanger arrangements of interest, and this frequently requires re-meshing of the arch when changing the number of hangers or the locations of their connection to the arch. In this context, it is noteworthy that preprocessing (including mesh generation) generally dominates the time spent for performing structural analysis.

- Transfer relations are *analytical* solutions of the underlying differential equations of the linear theory of slender circular arches, i.e. the computed solutions do not suffer from discretization errors. Therefore, there is no need for convergence analysis. This is different from discretization-based numerical solutions, where the same problem needs to be analyzed with meshes of different fineness, in order to be able to assess the discretization error. There is no need for such a convergence study if automatic remeshing based on error analysis is available which, however, is frequently not the case.

- Transfer relations are computationally inexpensive means to obtain a numerical solution of the given problem, because they always involve only a 7×7 transfer matrix (which is identical to the situation encountered in straight beams subjected to both axial loading and bending).

5. Conclusions

The following conclusions are drawn from this investigation:

- Transfer relations reduce the complexity of structural analysis of circular arches to the level of complexity of such analysis of systems consisting of straight beams.

- The transfer relations are attractive for sensitivity analysis regarding, e.g., the number of hangers of arch bridges, because the transfer relations can be easily specialized for different numbers of hangers.

- A uniform temperature change of 30 K causes rather small redistributions of internal forces but a significant change of the deformed configuration resulting from *dead load*. This is a consequence of the slenderness of the investigated arch.

References

[1] J. Cheng. Optimum design of steel truss arch bridges using a hybrid genetic algorithm. *Journal of Constructional Steel Research*, **66**(8–9): 1011–1017, 2010.
http://www.sciencedirect.com/science/article/pii/S0143974X10000775.

[2] C.L. Dym. End-loaded shallow curved beams. *Journal of Structural Engineering*, **137**(7): 782–784, 2011.
https://doi.org/10.1061/(ASCE)ST.1943-541X.0000396.

[3] C.L. Dym, I.H. Shames. *Solid mechanics: Variational approach*. McGraw-Hill, New York, 1973.

[4] C.L. Dym, H.E. Williams. Stress and displacement estimates for arches. *Journal of Structural Engineering*, **137**(1): 49–58, 2011. https://doi.org/10.1061/(ASCE)ST.1943-541X.0000267.

[5] G.F. Fox. Arch bridges. [In:] W.-F. Chen and L. Duan [Eds.], *Bridge engineering handbook*, chapter 17, pp. 17/1–17/12. Boca Raton, CRC Press, 1st edition, 2000. http://www.crcnetbase.com/isbn/9781420049596.

[6] J.M. Gere, B.J. Goodno. *Mechanics of Materials*. Cengage Learning, Stamford, CT, 8th edition, 2012.

[7] W. Hemp. Michell framework for uniform load between fixed supports. *Engineering Optimization*, **1**(1): 61–69, 1974. http://dx.doi.org/10.1080/03052157408960577.

[8] C. Melbourne. Design of arch bridges. [In:] G. Parke and N. Hewson [Eds.], *ICE Manual of Bridge Engineering*, pp. 305–344. London: Thomas Telford, 2nd edition, 2008.

[9] T. Mura. General theory of eigenstrains. [In:] *Micromechanics of Defects in Solids*, pp. 1–62. Springer, 1982. https://doi.org/10.1007/978-94-011-9306-1_1.

[10] Y.-L. Pi, M.A. Bradford. In-plane strength and design of fixed steel I-section arches. *Engineering Structures*, **26**(3): 291–301, 2004. https://doi.org/10.1016/j.engstruct.2003.09.011

[11] J. Salençon. *Handbook of Continuum Mechanics: General Concepts Thermoelasticity*. Springer, 2012. https://doi.org/10.1007978-3-642-56542-7.

[12] T.J.M. Smit. Design and construction of a railway arch bridge with a network hanger arrangement. Master Thesis, Delft University of Technology, Delft, The Netherlands, May 2013.
http://homepage.tudelft.nl/p3r3s/MSc_projects/reportSmit.pdf

[13] J. Wheeler. *An Elementary Course of Civil Engineering for the Use of Cadets of the United States Military Academy*. John Wiley & Sons, 1876.

[14] T. Yabuki, S. Kuranishi. An ultimate strength design aid for fixed-end steel arches under vertical loads. *Proceedings of the Japan Society of Civil Engineers, Structural Engineering/Earthquake Engineering*, **4**(1): 115–123, 1987. https://www.jstage.jst.go.jp/article/jscej1984/1987/380/1987_380_141/_pdf.

[15] J.-L. Zhang, C. Vida, Y. Yuan, C. Hellmich, H.A. Mang, B. Pichler. A hybrid analysis method for displacement-monitored segmented circular tunnel rings. *Engineering Structures*, **148**: 839–856, 2017.
https://doi.org/10.1016/j.engstruct.2017.06.049.